Low frequency noise measurements: applications, methodologies and instrumentation

C.Ciofi[*a], B.Neri[b]

[a]Dipartimento di Fisica della Materia e TFA and *INFM*, Salita Sperone,31 I-98166, Messina, Italy;

[b]Dipartimento di Ingegneria dell'Informazione,Via Diotisalvi,2 I-56100, Pisa, Italy

ABSTRACT

The analysis of the low frequency noise generated in solid state devices represents a key factor in the era of VLSI technology. This analysis is mandatory in order to obtain a characterization of the source of disturbances which cause a degradation of the signal to noise ratio. In fact, the increasing miniaturization level of modern integrated circuits leads to a significant increase in the noise to signal ratio, thus making noise one of the main limiting factors for pursuing the ultimate miniaturization limits. Moreover, as low frequency noise can be used as a probe capable of investigating the phenomena occurring at a microscopic scale, it can be useful for characterizing the quality and the reliability of microelectronic materials and devices. In the first part of this paper, as an example of possible applications, an overview of the utilization of Low Frequency Noise Measurement (LFNM) technique to the study of the most frequent causes of failure in integrated circuits and discrete components is presented and the need for purposely designed instrumentation for this type of study will be put in evidence. Starting from the examples presented in the first part, in the second part an overview of the instrumentation and procedures required to obtain a minimization of the background noise of the entire measurement system is presented. In fact, especially in the case of low frequency noise measurements (f< 1 Hz), the lack of standard, commercially available instrumentation characterized by the required sensitivity, may be one of the main obstacles to the utilization of LFNM technique. For this reason, a review of the most relevant results obtained by our research groups during the last few years in the design of dedicated ultra-low noise instrumentation and in the tuning up of the methodologies for the analysis of noise data, is presented.

Keywords: Noise Measurements, Spectral analysis, low noise instrumentation, electron device, reliability.

1.INTRODUCTION

Since the late 1960s, Low Frequency Noise Measurement (LFNM) technique has been used as a tool for the analysis of conduction mechanisms at a microscopic scale in solid state devices and for the characterization of the quality of electron devices and materials[1]. The most important peculiarities of LFNM technique are the following ones: i) it is not destructive, ii) it is highly sensitive to localized phenomena; iii) it does not require complicated procedures for the preparation of the samples and expensive instrumentation such as those normally used for microstructural analysis. However, a problem is sometimes encountered in the application of the technique: the lack of purposely designed instrumentation on the market. In fact, the sensitivity of LFN measurements depends on the background noise of the measurement chain and, in some cases, the level of background noise required by the application is not compatible with that of commercial instrumentation. This problem can be solved by using self made instrumentation, purposely designed for each specific application. One of the cases in which the LFNM technique can be advantageously used for a not invasive and not expensive analysis is the investigation of the most frequent failure mechanisms in electron devices. In fact, in most cases, the characterization of the reliability of ICs reduces to performing lifetime experiments in accelerated stress conditions and in an analytical extrapolation of the expected lifetime at normal operating conditions by means of rather crude models. The use of accelerated stress conditions, however, poses the important question whether the observed failures are due to the same mechanisms, which would be observed at normal operating conditions or are the result of different degradation mechanisms which show up because of the high temperatures and currents used during the reliability tests. On the other hand, using stress conditions close to the ones which will be experienced by the devices during their normal operation would lead to an unacceptable duration of the tests. Because of their high sensitivity to localized phenomena, LFNMs may prove a good candidate as a standard tool for the accurate characterization of the reliability of the future generations of ultra large scale integrated circuits. Several evidences of

[*] ciofi@ingegneria.unime.it; phone +39 90 676 5648; fax +39 59 391382;

the capability of LFNM to serve as a tool for the characterization of the reliability of electron devices are reported in the literature since '70[2,3] and a comprehensive review of the application of LFMN to the characterization of different failure mechanisms in electron devices can be found in [4] and in the references therein. Two specific examples will be described in section 2 and 3 of this paper. Besides, it must be noted that, while in many cases more and more sensitive instrumentation is required in order to perform meaningful conventional measurements on scaled electron devices (current-voltage characteristics or impedance measurements, for instance), the reduced cross section available for the current transport normally results in an increased level of noise superimposed to the average value of voltages or currents. In some cases, fluctuations comparable to the average values of the current have been observed in scaled devices[5] thus making the characterization of the low frequency noise performances of such devices mandatory, independently of the possible use of LFNM as a tool for the characterization of their reliability. Moreover, LFNMs can be regarded as a sensitive probe of the detailed motion of the charge carriers within a device and therefore it can provide invaluable information on the current transport mechanisms which can not be obtained by means of current-voltage measurements[6]. Particularly in the case of nanoscopic devices, noise measurements in general, and LFNMs in particular, are expected to provide useful insight in their conduction behaviour[7].

Unfortunately, notwithstanding the potential advantages of LFNMs based characterization techniques, their use is not yet as widespread as they would deserve. Sensible noise measurements, especially at very low frequencies (f< 1Hz), are not easily performed as several spurious effects often superimpose to the noise signal to be detected thus making the interpretation of the measurements result quite doubtful and questionable. Besides the external interferences which couple with the measurement chain which could be, at least in principle, completely removed by proper electrical, mechanical and thermal shielding, the instrumentation itself may become the limiting factor because it contributes with its own internal noise to set the minimum level of detectable signal. It must be noted that at very low frequencies thermal noise does not usually play an important role. It is the flicker noise ($1/f$ noise), particularly the one introduced by the active devices used in electronic instrumentation, which plays the most important role, thus making noise measurements at such frequencies quite challenging. Commercially available instrumentation, with rare exceptions, is characterized by a quite high level of flicker noise thus considerably limiting the field of application of LFNMs technique. This fact reduces the sensitivity of this analysis tool: the consequence is the need for over-biasing the Device Under Test (DUT) in such a way as to let it generate a sufficiently high level of noise. In the case of reliability studies, this would correspond to subjecting the DUT to higher and higher stress conditions, thus losing one of the potential advantages of LFNMs, that is the ability of obtaining sensible information at moderate stress conditions. This is the case, for instance, of the utilization of LFNM technique in the investigation of Electromigration in metal lines of IC[8] which will be described in section 2. In other cases, a high level of background noise of the measurement system may simply hide the occurrence of important charge transport mechanisms. This is the case, for instance, of the analysis of the precursory phenomena of the breakdown in thin oxide MOS capacitors[9] or the observation of RTS (Random Telegraph Signals) just before the occurrence of hard breakdown in these structures[10].

The feeling of our research group, in the past 15 years of experience in the field, is that a skill in the design and realization of low noise instrumentation with lower and lower level of background noise can represent a key factor for succeeding in the application of LFNM technique. In fact, many of the results which we have obtained are the direct result of the improvements in the design of the several pieces of instrumentation which contribute to setting the ultimate level of background noise in the measurement chain. In section 4 and 5, we will relate on the several issues connected with the realization of specific instrumentation for LFNMs and on the solutions which we have adopted for solving several specific problems which are normally encountered when dealing with such measurement technique. We trust that our experience in this field may serve as a source of useful suggestions for other researchers or, at least, as a reference for stimulating discussion on this quite fascinating topic.

2. ELECTROMIGRATION IN METAL LINES

Electromigration (EM) is one of the main causes of failure in IC. EM consists of the displacement of atoms from their position in the lattice caused by high current densities in metal lines. At current densities at which EM arises (j>2×10^6 A/cm^2), low frequency noise can be measured at the ends of the stripes. This phenomenon is called Electromigration Noise (EMN). The noise spectra are characterised by an $1/f^{\gamma}$ behaviour and the frequency exponent γ is the most significant indicator of the kinetics of the process. The existence of a correlation between $1/f^{\gamma}$ noise and

lifetime of metal stripes subjected to Electromigration (EM) is known since 1985[11,12]. The frequency exponent γ is an increasing function of the stress conditions (current density *j* and temperature *T*). Values of γ close to 2 indicate that the stress conditions are so weak that no observable damage will be caused during the measurement, whereas values of γ higher than 2.4 indicate that the line is experiencing quite hard stress conditions capable to cause irreversible damage in a few hours. When the stress conditions are such that the value of γ is close to 2, the following relationship is obtained[4]:

$$S_V = \frac{A}{f^2}\frac{l}{wt}\frac{\rho j^3}{kT}e^{-\frac{E_a}{kT}} \qquad A = \frac{(100\rho_s)^2}{n_a}\frac{4Z^* eD_0}{(2\pi)^2\lambda} \tag{1}$$

where *l*, *w* and *t* are the length, the width and the thickness of the line, ρ_s the resistivity/defect, *Z**e the effective ion charge, D_0 is the pre-exponential factor of the vacancy diffution coefficient, n_a the atom density and λ the vacncy mean free path. From the observed dependence of the power spectrum of the resistance fluctuations $S_R = S_V/I^2$ (*I* being the test current) on *T*, it is possible to construct an Arrhenius plot whose slope is proportional to the activation energy of the phenomenon. An example is shown in Fig. 1 in the case of Al-Si 1% lines[4]. This possibility is restricted to the case in which the γ is close to 2, otherwise the noise is no longer stationary and a lot of spurious phenomena can be observed which make the evaluation of activation energy E_a no longer possible. For this reason, the stress conditions have to be kept as moderate as possible: the consequence is that the level of EMN is quite low and, due to its frequency dependence, an Ultra Low Noise Amplifier (ULNA) with a low frequency limit of a few mHz has to be used. Amplifiers with this characteristics are not normally available on the market, therefore purposely designed instrumentation must be used.

In order to investigate the possibility of using LFNM technique for a fast evaluation of the lifetime of a set of stripes in EM regime, EMN measurements have been compared with lifetime obtained from resistometric tests. These tests consists of supplying the stripes with a fixed current and monitoring the resistance variations caused by the EM damage. In many cases, a correlation has been found[11,13-15] between EMN and lifetimes. In fact, it has been proved that, at least for samples made by the same material, the higher the noise, the shorter the lifetime. Moreover, it has been observed that not only the resistance, but also the EMN shows relevant modifications during the lifetime: the noise level increases by even more than one order of magnitude before any measurable change of resistance of the DUT is observed. This fact indicates the possibility of using the increase of the noise level as a failure criterion capable of displaying the early effects of EM damage. This can be done only by using purposely designed low noise data acquisition systems capable of monitoring EMN for hours, days and, depending on the stress conditions, even weeks. Data acquisition systems available on the market does not have the required sensitivity and a sufficiently low level of background noise, so that, also in this case, purposely designed instrumentation has to be used[16].

Another requisite of this long term noise measurements is the availability of a system for sample temperature setting compatible with the very low level of background noise of the measurement chain. Commercial ovens for lifetime tests are not suited for this application, therefore a temperature controlled sample holder, with proper shielding between the circuit driving the power in the heater, the samples and the low noise data acquisition system, should be used[17].

3. NOISE IN MOS JUNCTION AND DIELECTRIC BREAKDOWN

In modern VLSI circuits, metal oxides silicon structures whose dielectric thickness is a few nm are frequently used. These structures are subjected to the phenomenon of dielectric breakdown which can occur after a given time of stress at constant voltage. The causes which induce the degradation are not completely understood, and for this reason a great attention has been devoted to the investigation of the degradation mechanisms which occur in thin oxides (t_{ox}<10 nm). During constant voltage stress, two phenomena are observed before the final dielectric breakdown: SILC (Stress Induced Leakage Current)[18,19] and soft breakdown (SBD)[20-23]. They consist of a gradual (SILC) or sudden (SBD) modification of the I-V characteristics in the low field region. The occurrence of SBD can be put in evidence by performing real time LFNM, without interrupting the stress to measure the I-V characteristic. In fact, SBD cause an increase by orders of magnitude of the spectrum of the gate current fluctuations[24]. This phenomenon is probably due to the fact that a significant amount of the total current tunnelling through the oxide is concentrated in a small region in

which a localised lowering (weak spot) of the potential barrier has occurred. The most probable hypothesis for explaining these phenomena is that breakdown is triggered by a local increase in the current density due to a tunnelling assisted mechanism by the traps generated within the oxide layer and at the Si-SiO_2 interface[25] during the stress. The excellent sensibility to localised phenomena of LFNM technique makes it particularly suitable for this kind of applications[26-29] and can put in evidence phenomena that are neglected by using conventional techniques. In fact, these techniques, based on the utilisation of picoammeters or parameter analysers for monitoring the quantity under observation, are characterized by a low time resolution due to a quite narrow bandwidth: a few Hz as a maximum.

A typical behavior of the tunnelling current just before HBD is shown in Fig. 2: it consists of two levels or multilevel fluctuations of the current superimposed to an almost continuous value. The current pulses have an amplitude ranging from a few tens to a few hundreds picoAmperes and a duration ranging from a few milliseconds to a few tens of milliseconds. The experiment is realized using a dedicated low noise measurement system[30], whose block diagram is shown in Fig.3. Two independent inputs are available: one for the DC and another for the AC component of the signal, which require different data conditioning operations. As the observed current pulses show a duration from several milliseconds to hundreds of milliseconds, the AC channel bandwidth selected for this application ranges from 50 mHz to 1 kHz. A sensitive trigger system allows to stop the stress as soon as the PreBD current pulses start. Therefore, the test can be stopped prior to the catastrophic breakdown and an electrical and microstructural characterization of the silicon dioxide films close to the BD can be performed.

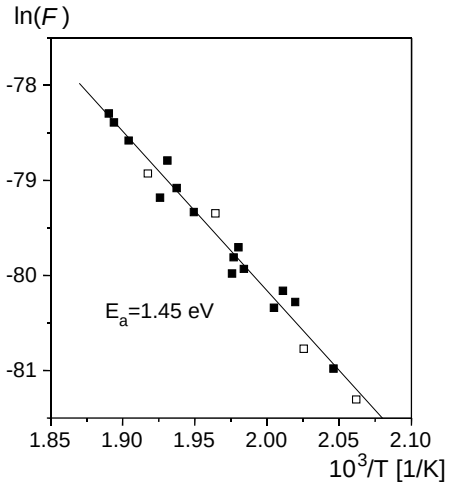

Fig. 1: Comparison between the behaviour described by Eq (1) (straight line), and the experimental points in submicrometric Al-Si lines with a bamboo-like structure. The quantity on the Y axes is defined as $F=S_R kT/(\rho j)$.

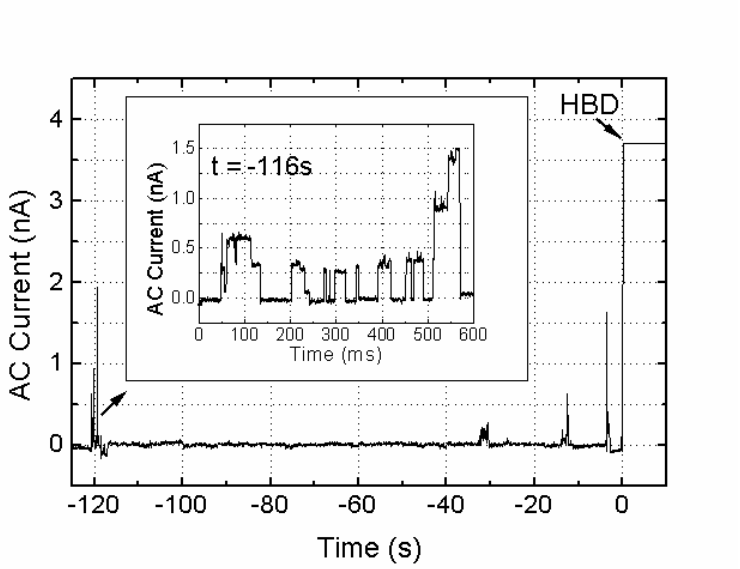

Fig. 2: Fluctuations of the current tunnelling through the dielectric of a thin-oxide MOS capacitor during a constant voltage stress. The breakdown occurred at t=0. A typical multistable behaviour of the current is shown in the inset in which the time interval around -116 s is zoomed.

The observed behaviour confirms the hypothesis that the phenomenon is correlated with the trapping-detrapping process of an electron by a trap located in a strategic position. Such a trap, by modulating the height of a potential barrier, could be capable of controlling a significant amount of the total current crossing the dielectric. The measurement system shown in Fig.3 has allowed to perform an interesting experiment: if the stress is stopped when the RTS fluctuations begin to show up, but the HBD has not yet occurred, the degradation of the dielectric layer can be partially recovered by means of thermal annealing[30].

Another application of LFNM in the investigation of the phenomena occurring in a thin oxide MOS devices is the characterization of shot noise of the gate current. In fresh oxide layers, the values of the DC current measured at different applied voltages coincide with the values expected for the pure tunneling current case and the power spectral density (PSD) of the AC current exhibits a white component, that results prevalent at frequencies higher than a few Hz. According to the hypothesis that the tunnelling of each current carrier is independent by that of the others, the current noise spectrum S_i shows a typical shot noise behaviour, that is $S_i = 2qI$ where q is the electron charge and I is the average value of the gate current. The situation changes after a high field stress (11 MV/cm): a SILC component of the gate current appears, and the spectrum S_i has a white component reduced value with respect to the case of the full shot noise. In Fig. 4 the Fano factor, i.e. the ratio between the measured spectrum of the SILC component and the corresponding full shot noise spectrum, is reported for different DC current values and for two different oxide thicknesses. It is observed that the noise spectrum of the SILC component is reduced by a factor of ~25% with respect to the case of the full shot noise[31]. The shot noise reduction clearly indicates some kind of negative correlation. On the basis of this observation, a few of the models proposed for SILC generation can be excluded, whereas the tunnel assisted model is confirmed since it can justify the existence of a correlation. In fact, a trap cannot contain more than one electron at a time, moreover the occupancy probability of a trap decreases if there are nearby traps occupied, because of Coulomb repulsion.

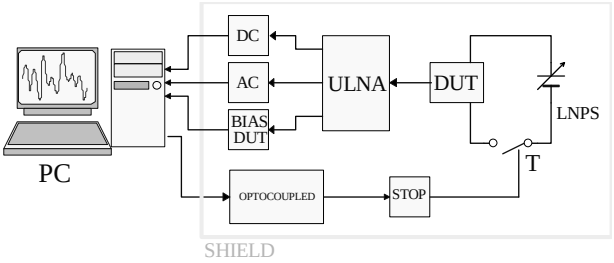

Fig. 3: Block diagram of the PC-based low noise measurement system

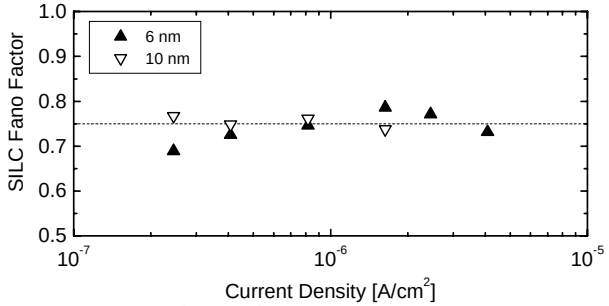

Fig. 4: Fano factor of the SILC component observed in stressed oxides at different DC current densities. A quite constant 0.75 value is observed in all our experimental conditions.

The case described in this section is a typical example of the new possibilities which are offered by the utilization of LFNM: the additional information which can be obtained can help, in a few cases, to discriminate among several possible interpretations of a phenomenon occurring at a microscopic scale and, in a few other cases, can be used to realize experimental procedure which could not be performed with traditional measurement setup.

4. INSTRUMENTATION

A simplified block diagram of the several pieces of instrumentation which make up almost any conceivable low frequency noise measurement system is reported in Fig. 5. It refers to the ideal and desirable case in which all the measurement parameters, especially the temperature of the thermal chamber and the bias level can be automatically set by means of an external controller, usually a Personal Computer (PC), in order to make it possible performing automated noise measurements. However, this is seldom the case in actual noise measurements, especially because although a few examples of low noise programmable, computer controlled, biasing sources have been demonstrated[31,32] their use is still limited either because of their size and high cost, or because of the complication involved in their integration as a standard piece of instrumentation in LFN measurement systems. Also a single power supply system as we have indicated in the figure is seldom present. Usually different set of high capacity batteries are used for providing both reference voltages and power supply for the most sensitive sections of the system. The use of batteries, besides providing a low noise power supply, allows to put them within the very same shielded enclosure which contains the DUT and the instrumentation, thus minimizing possible interferences coupling with the cables which need to cross the shield in the case in which the power is to be delivered from the external environment. However, batteries need to be frequently recharged, especially in the case in which they supply considerable current, as it is the case of delivering the

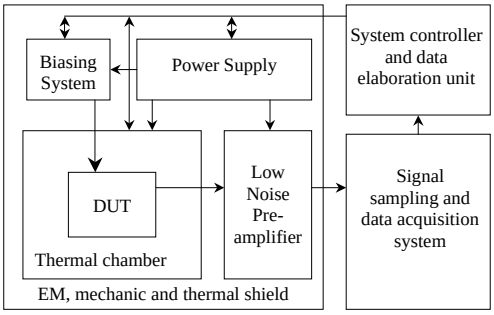

Fig.5: Block diagram of an automated LFNM system

power needed to supply the heathers of the thermal chamber. In such cases, unless one is willing to devise a shield capable of hosting very high capacity batteries, power must be delivered from outside the shield and possibly resorting to a solid state power supply. We will discuss the implications and problems of this approach later on in a paragraph dedicated to the design of a low noise thermal chamber. The signal sampling and acquisition unit often reduces to a standard Dynamic Signal Analyser (DSA). However, there are situations, such those corresponding to the case of a failure criterion based on long term noise measurements mentioned above, in which it may be desirable to store the entire time record of the detected signal in experiments which last several days. While it may appear that this could be easily done by resorting to a standard data acquisition board mounted on a PC, care must be taken in order to avoid that the interferences generated by the PC couple with the measurement chamber by way of the cables used for delivering the signal from the output of the low noise preamplifier to the input amplifier of the data acquisition system. The low noise preamplifier is certainly the most critical piece of the instrumentation of the entire measurements system, since it sets the ultimate limit of the background noise. However, it must be remarked that one can take full advantages of a low noise preamplifier provided that the other components such as the biasing system do not introduce too much noise. Moreover, there are techniques, which will be discussed in the following, that allow, in proper conditions, to reach a sensitivity which is well below that corresponding to the input equivalent noise of the amplifiers, and in these conditions the limiting factor may become the level of noise introduced by the biasing system, by the power supply system or the influence of external interferences. All these issued will be discussed in some detail in the following paragraphs.

4.1 INPUT PREAMPLIFIERS

By means of a careful design, the Equivalent Input Voltage Noise (EIVN) of a voltage amplifier may be reduced to the one introduced by the active device used for building up the first stage of the amplifying chain. In order to avoid disturbances coming from the power supply and other common mode interferences (temperature fluctuations, EM interferences and so on) the use of differential configurations is mandatory. As the best performances in terms of EIVN are to be found in discrete devices, we usually resort to a differential configuration with a discrete components input stage. In the course of our several experiments we have selected the matched BJT pair SSM2220 by PMI as the devices with the lowest level of EIVN (1.5, 3, 10 nV/[Hz]$^{1/2}$ at 1, 0.1, and 0.01 Hz, respectively). The complete schematic of the preamplifier is shown in Fig. 6[16]. A first pair of SSM2220 (Q1 and Q2) is employed to provide a low noise current bias for the differential pair (Q3 and Q4) which acts as the first gain stage of a differential high gain amplifier which includes a low noise OP27 operational amplifier (I stage). Note that all the resistors (save the high value resistors R2 and R3 in the second stage which are, however, crossed by very small currents) are metallic film resistors which are almost excess noise free. The first stage must be DC coupled to the DUT in order to supply the bias current required by the transistor Q3. This clearly sets a limit to the maximum value of the DC voltage which can be present at the input. As the overall gain of the amplifier is 80 dB, this would have resulted in a unacceptably low input dynamic range. It is for this reason that the gain of the first stage is limited to 30 dB and an ac coupling is provided from the output of the first stage to the input of the second stage with lower corner frequency of about 3 mHz. An AC coupling of the input with such a low corner frequency would not have been possible. In fact, in order not to introduce a considerable noise level due to the equivalent input current noise (EICN) of the BJT, we should have limited the value of the resistance of a *CR* high pass filter at the input to about 50 Ω and this would have required a coupling capacitor of about 1 F! As it can be noted in Fig. 6, the second stage has a JFET input which although characterized by a higher level of EIVN (the signal which reaches the second stage has been amplified by about 50) does require a very small biasing current (in the order of a few pA) and being characterized by a very low level of EICN does not introduce a significant amount of noise

notwithstanding that the resistance connected to its input has a value as high as 10 MΩ. With the approach we have followed, we obtain an input dynamic range of about ±100 mV. This may appear quite limited for many applications including the case of the EM experiments discussed above. However, measurement configurations as the one shown in Fig. 7, which specifically refers to the case of EM noise measurements, may be successfully employed. The dummy DUT may be an excess noise free resistor with a resistance value quite close to that of the sample and supplied with almost the same current, or may even be a second DUT nominally identical to the first one with the further advantage of doubling the voltage noise power at the input of the preamplifier. The dynamic range of the input is then sufficient for accommodating small tolerances in the value of the biasing currents and in the resistance values thus making the balancing of the system quite easy. When the equivalent impedance of the source is above a few tens of ohms, the effect of the high value of the EICN of the input BJT becomes predominant. In these cases a JFET input stage is preferable, although the best discrete devices we have been able to select for these applications (we currently use IF3601 discrete JFET by InterFet) have a significantly higher EIVN with respect to the SSM2220 devices. Since the required biasing current is in the order of a few pA, AC coupling down to the mHz range is readily obtained in the case of JFET input amplifiers. A JFET input low-noise amplifier can be realized using for the first stage a topology quite similar to the second stage of the amplifier in Fig. 6. A gain of 80 dB with a low frequency corner of about 3 mHz are easily obtained. When the performances of our amplifiers are compared to those of commercially available instrumentation, the improvement which can be obtained at very low frequencies is remarkable. As an example, the EIVN spectra of our BJT and JFET preamplifiers are compared to that of the popular Brookdeal 5003 in Fig. 8.

The case of transresistance amplifiers is somewhat different in that the main contribution to the output noise often

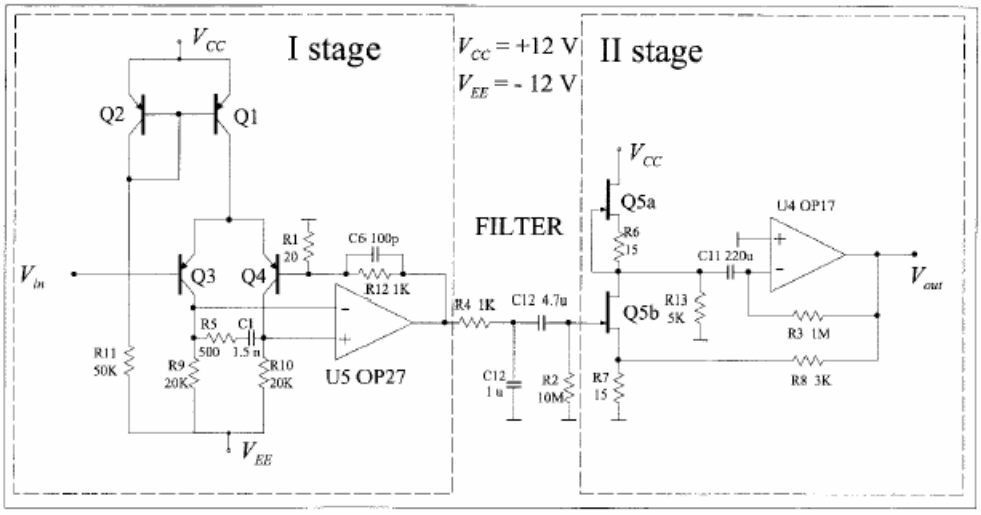

Fig. 6: Schematic of a BJT input ultra low noise preamplifier

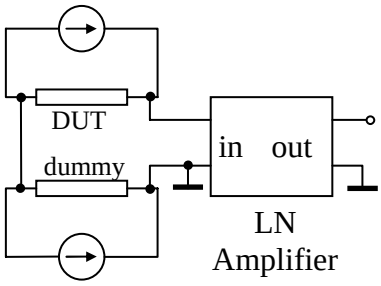

Fig. 7: Differential measurement configuration

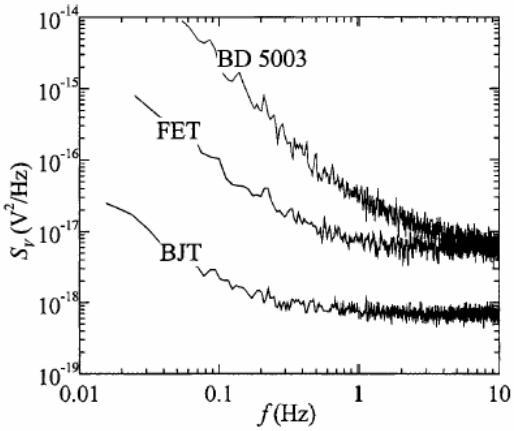

Fig. 8: Noise performances of different LN amplifiers

comes from the high value resistor which is used in a shunt parallel configuration for obtaining a high transresistance gain as in Fig. 9. In the figure, the equivalent input noise sources of the operational amplifier and the equivalent voltage noise source of the feedback resistor are explicitly shown. If the virtual short circuit approximation holds, the transresistance gain is equal to R_R and, in the case of equivalent impedance of the DUT much higher than the input impedance of the transresistance amplifier, the spectral density $S_{ineq}(f)$ of the equivalent input current noise source of the entire system can be estimated as follows:

$$S_{ineq}(f) = S_{in} + \frac{S_{vn}}{R_R^2} + \frac{4kT}{R_R} \tag{2}$$

In the case of a transresistance gain of 100 MΩ, one would obtain that the noise contribution due to the resistance R_R (the third term in Eq. 2) would amount to about 166×10^{-30} A^2/Hz. In order for the second term (noise due to the equivalent voltage input source of the operational amplifier) to be comparable with such a value, S_{vn} should be in the order of 1.6×10^{-12} V^2/Hz (that is 1.3 μV/[Hz]$^{1/2}$). This clearly demonstrates that for the realization of low noise transresistance amplifiers we must resort to operational amplifiers with a very low equivalent input current noise, while quite high values of equivalent input voltage noise can be tolerated. In our recent design we usually resort to the MOSFET input operational amplifier TLC070 which is characterized by an equivalent input current noise as low as 3.6×10^{-31} A^2/Hz notwithstanding that the equivalent input voltage noise is quite high (90 nV/[Hz]$^{1/2}$@1 Hz). Eq. 2 also shows that increasing the feedback resistance is beneficial as far as the equivalent input noise is concerned. However, there are limitations to the value R_R can assume. First of all, it is sometimes difficult to AC couple the device under test to the input of the transresistance amplifier and therefore the DC component of the current must flow across R_R without saturating the output stage of the operational amplifier. Moreover, the bandwidth of the amplifier is often limited by the

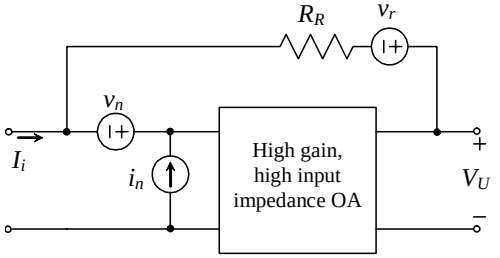

Fig. 9: Simplified schematic of a transresitance

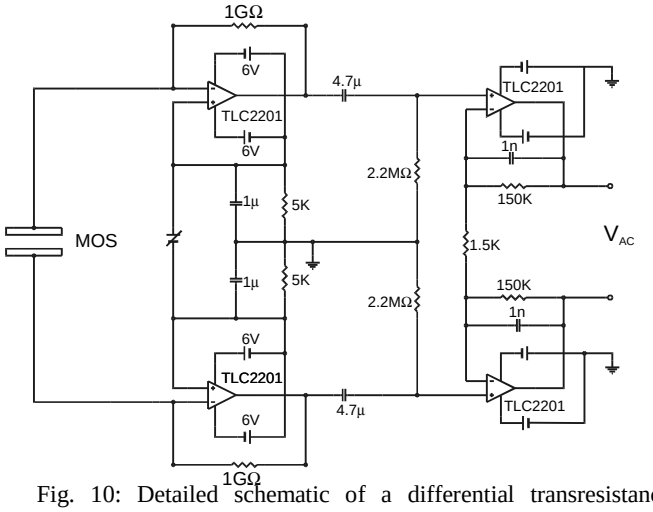

Fig. 10: Detailed schematic of a differential transresistance amplifier used for MOS noise characterization

parasitic capacitance in parallel to R_R itself. Since for a given resistor technology and package such a capacitance is almost independent of the resistance value, the bandwidth decreases proportionally to R_R. In some cases a differential arrangement such as the one reported in Fig. 10 may be used. The case shown in the figure refers to the study of the current noise spectra of stressed and unstressed thin oxide MOS devices. The biasing of the DUT is obtained taking advantage of the virtual short circuit at the input of the two identical transresistance stages, with the reference battery not supplying current, save the very small one needed for biasing the inputs of the operational amplifiers (in the order of 1 pA for the TLC070); the DC value of the differential voltage at the output of the two transresistance stages can be used for monitoring the current flowing through the DUT; the transresistance gain is doubled with respect to the case of a single transresistance stage (and therefore the amplification of the input noise spectra is increased by a factor 4), while the output noise spectrum, because of the incorrelation between the equivalent voltage noise sources of the two feedback resistances is just doubled. Therefore an equivalent reduction of a factor 2 is obtained in the equivalent input background noise of the system.

The observation that the background noise of a transresistance amplifier is mostly due to the feedback resistor used for realizing a high transresistance gain, has recently lead us to explore the possibility of designing transresistance amplifiers which used a noiseless impedance in the feedback loop rather than a resistance. This could be done in principle by employing a feedback capacitor instead of the resistor R_R in Fig. 9. This idea has lead us to the design of a new topology for the realization of a high gain, low noise, high bandwidth transresistance amplifiers. The schematic of the new topology is reported in Fig. 11. The resistor Rc_1 is required to provide a feedback path in DC for the first operational amplifier. The condition $Rc_1 \times C_1 = Rc_2 \times C_2$ must be satisfied in order to have a flat response down to DC. In the virtual short circuit approximation, the transresistance gain A_{R0} results:

$$A_{R0} = \frac{C_2}{C_1} R = 100\ M\Omega \tag{3}$$

It can be demonstrated[32] that the new approach allows, for the same value of the transresistance gain, to obtain an increase of the bandwidth by a factor C_2/C_1 and a reduction of the EICN by the same factor. This last advantage can be obtained in the case in which the resistance R_{C1} can be made large enough not to contribute significantly to the output noise. A comparison between the performances which can be obtained by using the new approach with respect to the conventional one (for the same transresistance gain and using the very same operational amplifiers and resistance types) is given in Fig. 12. As it can be noted form Fig. 12a, the output noise in the case of the new approach start to increase with respect to the value at very low frequencies at about 1 kHz. This is due to the combined effect of the EIVN of the operational amplifier and the common mode parasitic input capacitance of the operational amplifier. The same effect is present in the conventional design, but it is hidden because of the limited bandwidth and the much higher level of white noise. This is clearly shown in Fig.12b, where the calculated EICN power spectral densities (using the exact expressions of the transresistance gains) are reported.

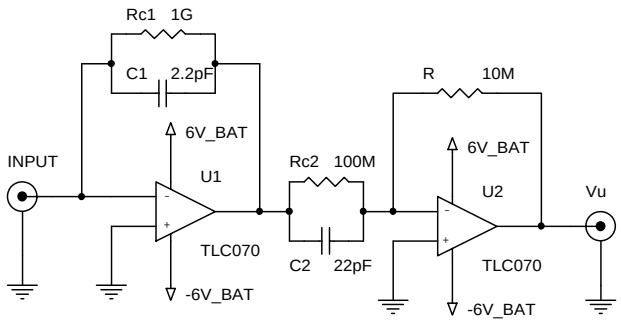

Fig. 11: New topology for a low noise, high bandwidth

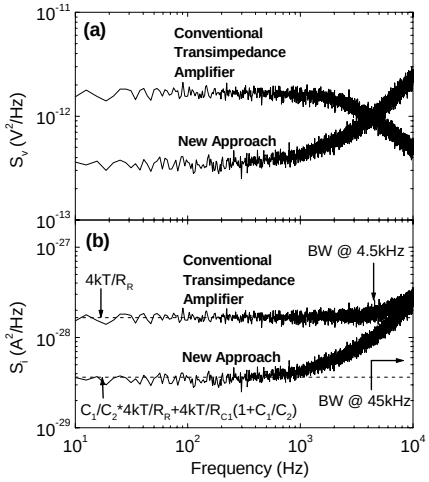

Fig. 12: Comparison of the noise performances between the new and the conventional transresistance

4.2 BIAS SOURCES

Solid state voltage or current sources are normally useless in the case of LFNM because of the high level of 1/*f* noise produced by the zener device which is used as a voltage reference in all these systems. Therefore, high capacity batteries are normally used for providing voltage bias to the DUT. Current bias is obtained by batteries as well by connecting a few batteries in series and using a conveniently large series resistor. Batteries behave as low frequency noise voltage or current sources provided that they do not supply too much current. As a rule of thumb (for measurements down below 100 mHz) it must be avoided any situation in which the battery supplies a current as high as

needed to fully discharge it in less than 100 hours. In any case, the voltage or current supplied by a battery drops with time depending on the supplied current and therefore it is never the same in repeated measurements. Moreover only a discrete set of voltages are available which are an integer multiple of the cell voltage. One can resort to resistive voltage dividers, but in this case, for the system to behave as a low internal resistance voltage source, the current supplied by the battery must be quite large thus making the problem of the discharge more and more important. Remote control of the voltage value is not possible and therefore a lot of time is wasted in manually changing the configuration of the battery packs in order to obtain a voltage as close as possible to the desired one or for just monitoring the actual value of the supplied voltage. The problem of realizing reliable voltage or current sources (either programmable or not) is never an easy one because the level of noise introduced by such devices directly appears at the ends of the DUT which is clearly the most sensitive part of the measurement system. In the course of the last few years we have addressed the problem of the realization of fixed and programmable voltage or current sources and we believe that some of our results are remarkable and deserve to be mentioned here.

4.2.1 Fixed value low noise voltage and current sources.

We start from the observation that almost any battery, when supplying a very low current, may behave as a very low noise, high stability voltage reference. In fact, while the exact value of the generate voltage does depend on the charge state of the batteries (for rechargeable batteries) or on their age (for non rechargeable ones), if the battery does not supply current, such a value may be assumed almost constant for a long period of time. Accurate measurements performed in a highly stabilized temperature chamber (30 $\pm$0.005 ^{O}C) have shown that the voltage drop (mainly due to self discharge) is in the order of 100 ppm/h in the case of lead acid batteries (Sonnenschein Dryfit A300, 6.8 V, 1.1 Ah), while in the case of non recharghable lithium batteries (Duracell type 223, 6 V) the voltage drift can be as low as 3 pmm/h. Even in the case of the lead battery, the voltage drift results 14 mV in 24 hours which is largely acceptable for many applications. The rate of self discharge is not usually reported by the manufactures, however there is a strict correlation with the shelf life: the longer the shelf life, the lower the voltage drift rate. A simple circuit which behaves as a low noise voltage source is illustrated in Fig. 13. The high value resistor R in series with the battery is necessary in order to avoid that the battery discharges when V_{DD} is turned off. The capacitor C is then required for filtering out the thermal noise generated by the resistor. With a careful design of the RC time constant, the power spectrum of the voltage fluctuations at the output of the system reduces to that introduced by the EINV source of the JFET device. The resistance R_D is needed in order to maintain the drain-source voltage below the value for which impact ionisation in the channel becomes significant. In fact, as impact ionisation becomes significant, the current through the gate and the associated current noise increases as well. When employing the large area JFET IF3601 by Interfet, voltage noise as low as 5×10^{-15},10^{-16}, 10^{-17} V^2/Hz at 10 mHz, 100 mHz and 1 Hz, respectively, can be obtained. In the case in which very high stability is required, care must be taken in order to avoid the influence of temperature changes which cause changes in the voltage generated by the battery and in the value of the V_{GS} voltage of the JFET. The temperature dependence of the V_{GS} of the JFET can be as high as 2 mV/^{O}C, and therefore accurate thermal shielding is required. At the same time, the JFET must be allowed to easily dissipate the heat generated during its operation. We usually resort the expedient of enclosing the JFET in a massive brass holder (100-200g) entirely surrounded by a thick PTFE enclosure. In this way, notwithstanding the high value of the thermal resistance provided by the PTFE layer, the large exchange area allows for sufficient heat transfer. Using a battery as a reference, we can also realize a low noise current source using the configuration reported in Fig. 14. Here the reference battery together with the source resistance R_S sets the current value according to the following equation:

$$I_{OUT} = \frac{V_B - V_{GS}}{R_S} \tag{4}$$

Using values of V_B in the order of a few volts (for instance 6 V by employing a lead acid battery) one may neglect, as a first approximation, the value of V_{GS} which can be in the range of a few hundreds of volts in the case of the IF3601. By neglecting the contribution of the noise produced by the battery and by the resistance R (the thermal noise produced by the resistance R is filtered out in the bandwidth we are interested in by a proper choice of the capacitor C), the power spectral density of the current fluctuations delivered to the load can be estimated as follows:

$$S_{Iout} = \left(S_{enFET} + 4kTR_S\right) \times \left(\frac{g_m}{1 + g_m R_S}\right)^2 \tag{5}$$

where S_{enFET} is the power spectral density of the equivalent input noise voltage of the JFET and g_m is the transconductance corresponding to the operating point of the JFET. When employing the large area JFET IF3601, transconducances in the order of a few hundreds of mA/V are easily obtained and, therefore, for resistances R_S higher than 100 Ω one has $g_m R_s >> 1$ and the previous equation can be simplified as follows:

$$S_{Iout} = S_{enFET}\left(\frac{I_{out}}{V_B}\right)^2 + 4kT\left(\frac{I_{out}}{V_B}\right) \tag{6}$$

In the case of currents below 50 mA and assuming V_B=6 V, the term $4kTI_{out}/V_B$ is below 5×10^{-22} A^2/Hz and it can be shown to become negligible with respect to the first term in the frequency range below 0.5 Hz. The actual circuit used for realizing a practical low noise current noise source is actually more complex with respect to the one shown in Fig. 14, because, as in the case of the voltage sources, we must avoid too large values of V_{DS} independently of the particular value of the load impedance Z_L. The circuit we normally use is described in detail in reference[33]. In such a circuit, two IF3601 JFET are used in parallel in order to achieve a maximum current output of about 100 mA without causing excessive heating of the transistors. The current to be supplied can be changed by changing the value of the source resistances (one for each JFET) according to the equation given above. As an example of the noise performances which can be obtained using this current source, the power spectra of the current fluctuations at its output are reported in Fig. 15 for different values of the current (IGEN in the figure) supplied to a 200 Ω resistive load. Such a current source has been successfully used to demonstrate the feasibility of low noise measurements on metallic interconnections at wafer level[34].

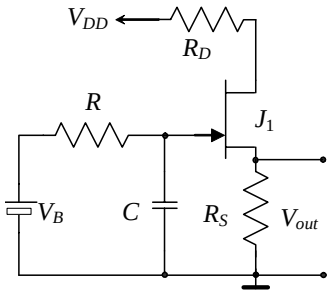

Fig. 13: Schematic of a LN fixed voltage source

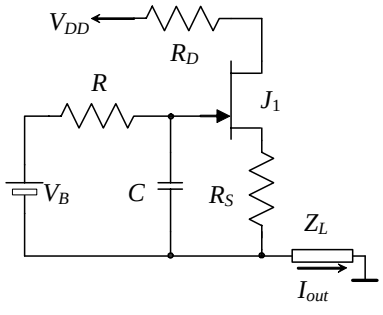

Fig. 14: Schematic of a LN fixed current source

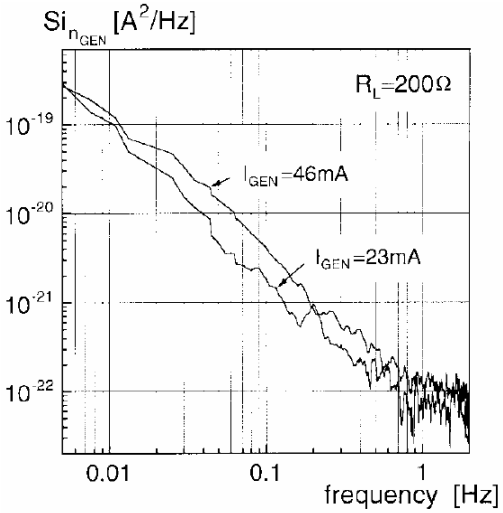

Fig. 15: Current noise t the output of an ultra low noise current source

4.2.2 Programmable low noise voltage sources

Designing programmable (that is remote-controlled) low noise voltage or current sources is not an easy task. Standard DA converters produce a high level of low frequency noise and cannot be used to directly provide a programmable voltage to be used instead of a battery in circuits such as those reported in Fig. 13. Moreover, the digital circuitry needed for the operation of such programmable sources is likely to introduce interferences which would degrade in any case the noise performances of the system. Up to now we have however successfully addressed the issue of designing and realizing programmable, high accuracy, ultra low noise voltage sources. Such pieces of instrumentation could be used to replace the reference battery used in low noise fixed current noise sources thus changing them in programmable

current sources. As yet, however, we have not thoroughly addressed this last issue and the discussion here will be limited to the case of programmable low noise voltage sources. We have experimented two different solutions for the realization of low noise high precision programmable voltage sources. In one case[35], we used a low noise fixed value voltage source as a reference for a low noise resistive voltage divider ladder network. The output of such a ladder network was used as the input of a low noise power voltage follower to provide low output impedance and high current driving capability. A block diagram of such a programmable low noise voltage source is reported in Fig. 16. The low noise resistive ladder network is realized using excess noise free metallic film 1% resistors and a set of low contact resistance miniaturized relays. In order to obtain high accuracy notwithstanding the high tolerance of the resistors of the ladder network and the uncertainty in the actual value of the low noise fixed voltage source (the exact value of the supplied voltage depends on the actual value of the reference battery voltage which drifts with time) the Static Analog Memory (SAM) concept, developed by our group[36,37] has been implemented. When the output voltage need to be changed, the switch S_1 is brought in position 2 by the microcontroller (μC), the voltage to be generated is set at the output of a high accuracy (but noisy) solid state DA converter and an automatic approximation procedure is started by the μC which allows to obtain at the output of the discrete $R/\beta R$ ladder network a voltage as close as desired to the one generated at the output of the solid state DA converter. The possibility of obtaining high accuracy notwithstanding the high tolerances of the resistors employed in the discrete ladder network and the uncertainty in the actual value of the output of the fixed value low noise voltage reference is guaranteed by design by selecting a proper value of β (β>2). When the approximation procedure ends, the switch S1 is brought back in position 1 and the new programmed voltage value is obtained at the output. The capacitors C is used in order to maintain the output voltage constant during the approximation procedure needed to change the voltage at the output of the discrete ladder network. An optoisolated RS232 interface is used to remote control the instrumentation by means of an external PC. The instrumentation behaves as a very low noise 12 bit DA converter capable of generating voltages in the range from 0 to 8 V with an accuracy better than ±1.5 mV and delivering to the load currents in the range of a few hundred mA. Typical values of the spectral density of voltage fluctuations at the output are 10^{-12}, 10^{-15}, 10^{-16} V^2/Hz at 0.01, 0.1 and 1 Hz, respectively.

As a second possibiliy, we have verified the possibility of realizing a programmable low noise voltage reference by directly filtering the output noise of a standard solid state DA converter. With reference to Fig. 17, if the time constant of the RC filter in the figure is chosen sufficiently high, the high level of noise produced by a standard solid state DA converter (more than 50 dB above that corresponding to the EIVN of the IF3601 in the frequency range below 1 Hz) could be filtered out starting from a conveniently low frequency. However, it may be calculated that at f=100 mHz, in order to reduce the noise generated by a "low noise" commercial DA converter (in the order of 10^{-10} V^2/Hz at 100 mHz) to a level at least 10 dB below that of the EIVN of the JFET ($10^{-16}V^2$/Hz at 100 mHz), a time constant of about 30 minutes would be required, thus making the use of the device impractical because one would have to wait a few hours

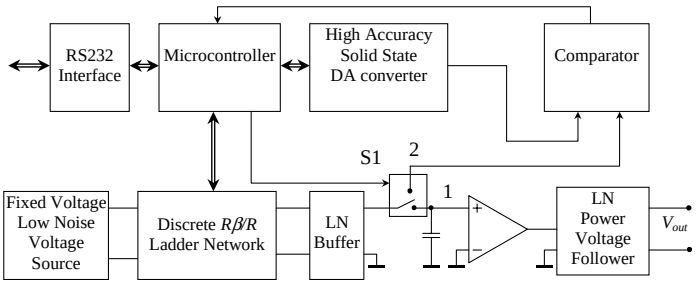

Fig. 16: Block diagram of an ultra low noise programmable voltage source

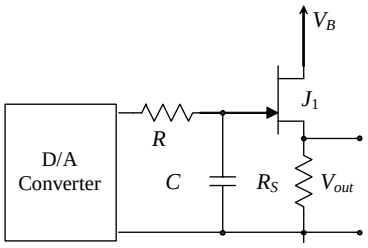

Fig. 17: A simple implementation of a low noise

before having a stable output upon any change of the voltage to be generated. In order to overcome this limitation, we resorted to the circuit shown in Fig. 18 which is part of a microcontroller based control system[38]. The optically controlled analog switch (H11F1) behaves as a very high resistance with the driving LED switched off (Roff>300 MΩ), while it behaves as a small valued resistance when the LED is turned on. The driving LED may be automatically operated by the microcontroller, being switched ON in order to speed up the voltage change transient. When the new steady state condition is reached, the LED is switched off in such a way as to allow the low pass filter to develop its full action. In fact, while the output voltage is changing, no noise measurement would be meaningful and by means of the procedure described above, the new steady state is reached in a matter of a few minutes. We decided to employ two

high capacity 12 V, 6Ah lead acid battery, one for the control board and one for the output buffer, in order to reduce the size of the entire system. For the output voltage to reach 0 V we had to insert the battery V_{B1} which insures that the JFET is pinched off when the input voltage is close to 0 V. At the same time the battery allows, together with the darlington Q1, to maintain the JFET in saturation with the lowest possible value of V_{DS}. The battery V_{B1}, through which only the negligible gate current flows, is obtained as the series of 3 tiny 100 mAh NiCd cells. The noise performance which can be obtained are impressive as can be noted from Fig. 19. In the figure, together with the power spectrum of the voltage fluctuations *Sout* measured at the output of the voltage source we have reported the power spectrum of the voltage fluctuations of the solid state voltage source (REF192) which provides the reference for the DA converters. The curve labeled SBN is the background noise of the measurements system. Accuracy and stability of the supplied voltage are within ±250 μV in the entire output voltage range.

4.3 LOW NOISE THERMAL CHAMBER

In some cases, LFNMs must be performed on samples maintained at a fixed temperature. This is certainly the case for the characterization of the electromigration in metal lines. Commercial thermal chambers as those used in standard reliability test cannot be used because of the high level of temperature fluctuations and the low shielding from external interferences. In the past we have been using custom miniaturized heather that were battery supplied in order to be able to put them in the shielded measurement environment. Moreover, using batteries avoided the thermal fluctuations induced by the voltage fluctuation of solid state power supply. More recently, because of the need of a thermal chamber

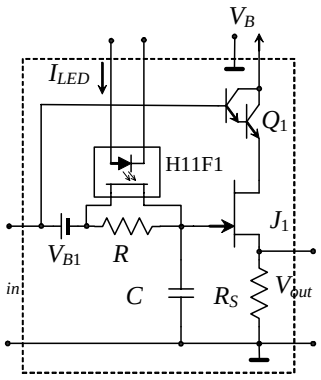

Fig. 18: Improved filter stage for the realization of a low noise programmable voltage reference

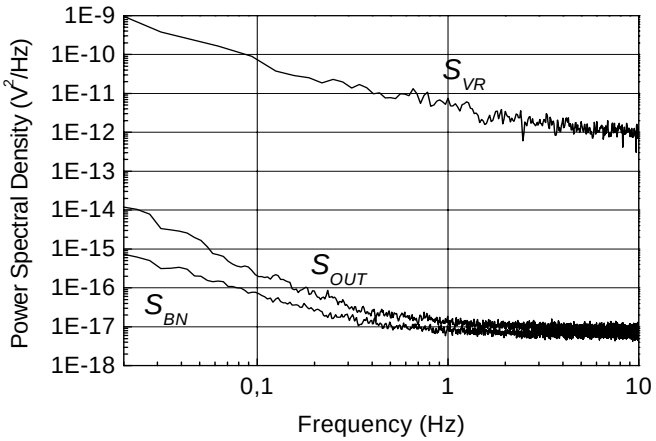

Fig. 19: Noise performances of the digitally programmable low noise voltage source. SBN is the background noise of the measurement system, Svr is the noise of the solid state voltage reference of the DA employed in the design.

large enough for hosting several samples and with the capability of allowing very long autonomy for performing long term noise measurements[39], we had to face the problem of the design of a high stability thermal chamber capable of meeting these requirements. In a thermostatic chamber, the residual thermal fluctuations are primarily due to two sources: the environmental perturbations and the fluctuation of the power source which supplies the heater. If we assume that the temperature dependence of the samples (metallic stripes) to be held in the thermal chamber at constant temperature and supplied with a constant current *I* is as follows:

$$R_S = R_0\left(1+\alpha\left(t-T_{0'}\right)\right) \tag{7}$$

where R_0 is the value of the resistance at the reference temperature T_0 and α is the temperature coefficient of the resistance, it can be easily estimated that the voltage fluctuations at the ends of the samples caused by the thermal fluctuations is given by:

$$S_v = S_T \alpha^2 R_0^2 I^2 \tag{8}$$

where S_T is the power spectral density of the temperature fluctuations inside the sample chamber. For typical values of the parameters appearing in the previous equation ($\alpha=4\times10^{-3}K^{-1}$, $R_0=100\ \Omega$, $I=100$ mA) we have that, in order to obtain S_v lower than that corresponding to the background noise of the best low noise preamplifier we have available(10^{-16} V^2/Hz at 10 mHz), the power spectrum of the voltage fluctuation S_T must be below 10^{-12} K^2/Hz. Using standard solid state power supplies, it may be calculated that the amount of metal which would be needed for realizing a thermal capacitance sufficient for filtering out the temperature fluctuations induced by the power supply fluctuations, would be impractical. In the case of our design[17], in order to improve the temperature filtering effect, the choice has been made to use a two stage thermal structure in which two coaxial aluminum vessels are separated by a thermal insulating layer (PTFE). This structure, shown in Fig. 20, acts as a second-order low-pass filter, effectively reducing the effects of environmental perturbations. When compared with the single-stage traditional structure, this solution has proven to be much more effective (more than 90 dB in reducing thermal fluctuations with respect to an oven chamber of equivalent dimensions and using the same mass of aluminum). The sample chamber can reach a maximum temperature of 250 ^{0}C with a stability better than 0.1 ^{0}C. The effectiveness of the design was such that we were not able, using the best instrumentation we had available, to evaluate the residual thermal fluctuations within the sample chamber[17]. The internal heater directly in contact with the inner chamber (Fig. 20) is supplied only during start up in order to reduce the time required for reaching a steady state temperature in the sample chamber.

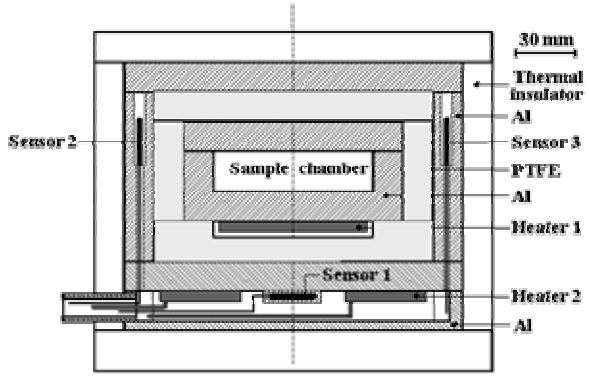

Fig.20: Double stage thermal chamber for LFNM

5. SIGNAL ACQUSITION AND ELABORATION

Noise spectra estimation in the case of LFNMs is usually performed by resorting to dynamic signal analyzers which essentially numerically perform the FFT of sufficiently long time records. The use of commercial FFT spectrum analyzers has, however, a few limitations. Usually only one or two input channels are available thus making the possibility of using LFNMs for performing reliability tests on a large number of samples[39] either impossible or time consuming because of the need of testing at most two samples at a time. Usually, after performing the calculation of the FFT, the acquired time record is discarded to make room for another one. While this may not be a limitation in the case of measurements lasting a few minutes, when we remember that, in order to perform sensible noise estimation of power spectra down to a few mHz a time record of several thousands of seconds need to be elaborated, not to talk of the case of long term noise measurements[39], a few drawbacks arise. In the first place, it is seldom possible for an operator to constantly monitor the measurement in order to detect possible interferences which although causing a large increase in the measured spectra may have nothing to do with the noise being monitored. Therefore, in the case of unusual large spectra, the only option for confirming the correctness of the result is to repeat the measurement, which is of course quite annoying and time consuming. Moreover, as any commercial FFT analyzer work on a time record containing a given maximum number of samples (say a few thousands) one has to make the choice, at the beginning of the measurements of either privileging frequency resolution at the cost of bandwidth or of privileging bandwidth at the cost of resolution. If one realizes that a different bandwidth-frequency resolution combination was necessary, the only possibility is to repeat the measurement with the new parameters. All these problems would be solved if it were possible to store the entire duration of the time record in such a way as to be able to defer the spectral estimation at the conclusion of the measurements. In this way, one could play back the acquired data at a faster speed and make sure that

no anomalous behavior occurred during the measurements. Moreover one could make the spectral estimation using different combinations of bandwidth and frequency resolution without the need to start a new measurements. We have in fact designed and realized such a system which, in its early version was described in reference [34]. The system we use at present is based on a DSP board that we have purposely developed for LFNMs and uses a PC for controlling the acquisition, storing the data and performing spectral estimation. The system has 8 input channels and behaves, during the measurements, just as a conventional 8 channel FFT would do (displaying the acquired signals in the time domain and performing spectral estimation on line), save that the time records acquired during the measurements are entirely stored and can be played back at will after the completion of the measurements. The maximum acquisition frequency is 512 Hz, which is largely sufficient for LFNMs. For the connection from the front end and the sampling boards to the PC, we used a fiber optical link in order to avoid the electromagnetic interferences generated by the PC to reach the low noise preamplifiers.

Signal elaboration, either before or after sampling, may be useful not only for simplifying the execution of sensible LFNMs, but also, in proper conditions, to reach equivalent background noise which may be below that of the input preamplifiers used for the measurements. The possibility of performing reliable noise measurements when the noise produced by the DUT is comparable to, or even much lower than, the background noise of the input preamplifier has been demonstrated using different methods[40-42]. These methods take advantage of the uncorrelation of the noise sources of the measurement chain with the noise produced by the DUT. In a recently proposed approach, two independent amplifiers are connected to the DUT[41] and a two channel Discrete Fourier Transform (DFT) processor is used to numerically estimate the cross spectrum of the signals at the output of the two amplifiers, with the result of eliminating most of the contribution of the noise introduced by the amplifiers. We have recently proposed another method for performing reliable very low noise measurements which, although in principle equivalent to the one just described, is based on a rather different approach. The circuit configuration of the proposed high sensitivity measurement system is reported in Fig. 21 for the case of voltage noise measurements. The DUT voltage noise V_s is simultaneously amplified by two different channels with identical gains and the two amplified signals are fed to the analogic addition and the subtraction blocks. The output voltages $x_1(t)$ and $x_2(t)$ can be written as:

$$\begin{cases} x_1(t) = c(t) + u_1(t) \\ x_2(t) = c(t) + u_2(t) \end{cases} \tag{9}$$

where $c(t)$ is due to the input signal and to the equivalent input current noise (EICN) of the two amplifiers, $u_1(t)$ is due to the equivalent input voltage noise (EIVN) of the first amplifier and $u_2(t)$ is due to the EIVN of the second amplifier. Therefore, at the output of the addition and subtraction blocks we have:

$$\begin{cases} a(t) = 2c(t) + u_1(t) + u_2(t) \\ s(t) = u_1(t) - u_2(t). \end{cases} \tag{10}$$

At least in the case of low frequency noise measurements, one can assume that $u_1(t)$, $u_2(t)$ and $c(t)$ are uncorrelated and, therefore, at the output of each channel of the spectrum analyzer in Fig. 21 we have:

$$\begin{cases} S_a(f) = 4S_c(f) + S_{u1}(f) + S_{u2}(f) \\ S_s(f) = S_{u1}(f) + S_{u2}(f) \end{cases} \tag{11}$$

where $S_x(f)$ is the Power Spectral Density (PSD) of the signal $x(t)$. By subtracting $S_s(f)$ from $S_a(f)$ we obtain an estimate of $S_c(f)$ alone. It is clear that, in the frequency range in which the contribution of the EICN of the amplifiers is negligible, we obtain a direct estimate of the PSD of the noise signal we are interested in. Since the contributions of the EIVN of the amplifiers cancel out, the sensitivity of the measurement method is limited by the contributions of the EICN, whose effect depends on the equivalent impedance of the DUT. This fact implies that in order to measure very low voltage noise, the EICN of the amplifier represents the limiting factor rather than the EIVN. Therefore, using the measurement configuration we propose, one may obtain better noise performances from MOSFET input stage amplifiers (high EIVN and low EICN) rather than from those employing BJTs (low EIVN and high EICN), even in the case of low DUT impedances. Besides resulting in many cases in a simpler implementation with respect to others, our method does not depend on the properties of DFT based spectrum analysis and can be successfully performed even by

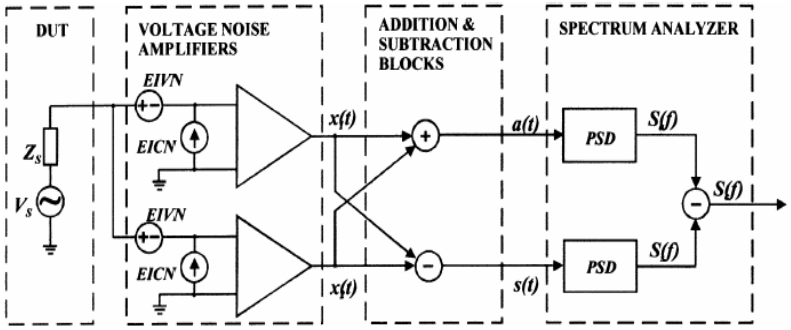

Fig. 21: Block diagram of the new voltage noise measurement system

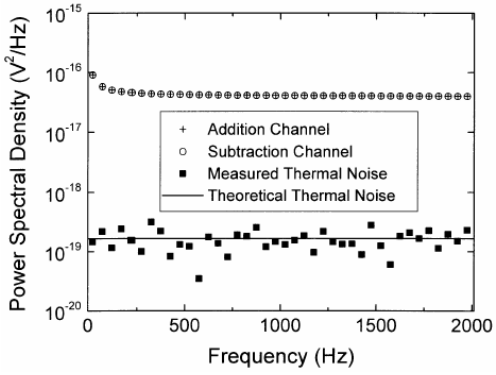

Fig. 22: Power spectra at the output of the adding and subtracting channel and estimated spectrum of the input voltage noise

using a single channel spectrum analyzer. In fact, one can evaluate the PSD of the *a* channel alone, then that of the *s* channel alone, and finally perform the subtraction of the two PSDs thus obtained. In order to verify the effectivenes of our approach, we used two voltage noise amplifier based on the TLC2201 by Texas Instruments, which is characterized by a relatively high EIVN (10 nV/√Hz, f>100 Hz) and by an excellent level of EICN (0.6 fA/√Hz). Two INA141 instrumentation amplifier were used for realizing the adding and subtracting blocks. We measured the PSD of the voltage fluctuations at the outputs of the addiction and subtraction blocks by means of a dual channel FFT spectrum analyzer based on a National Instruments PCI-4451 board. A resistance R_{10} of 10 Ω was used as DUT. It acted as a source of voltage noise with a power spectral density of $4kTR_{10}$, where k is the Boltzmann constant and T is the absolute temperature. At room temperature the value of the PSD of the voltage fluctuation to be measured is about 407 pV/√Hz. As it can be verified in Fig. 22, the estimation of the PSD of the voltage fluctuations at the ends of R_{10}, as obtained by using the proposed method, is rather good, with an average value of 409 pV/√Hz and a standard deviation of 270 pV/√Hz after 2^{16} averages with a frequency resolution of 25 Hz, within the investigated bandwidth. It must be noted that the noise produced by the DUT is, in the low frequency range of the spectrum, almost 30 dB below the EIVN of the input amplifying stages. We have also demonstrated the effectiveness of the new method also in the case of current noise measurements, and an example of the results which can be obtained can be found in reference [43].

6. CONCLUSIONS

In this paper we have discussed the application of LFNMs to the characterization of the quality and reliability of electron devices. The need for purposely designed very low noise instrumentation has been put in evidence. Some of the most interesting results obtained by our groups both in the field of the application of LFNMs to the characterization of electromigration and thin oxide breakdown and in the field of the design of ultra low noise instrumentation have been reviewed. Our experience is that there has always been a sort of regenerative feedback between the improvement of the performances of the instrumentation and the extension of the field of application of LFNMs: the better the instrumentation, the deeper the understanding of the phenomena being investigated. It is for this reason that we strongly feel that a closer collaboration between research groups interested in the application of LFNMs and research groups involved in the design of low noise instrumentation may prove an important step toward the diffusion and the standardization of this technique.

REFERENCES

1. F N Hooge and A M Hoppenbrouwers, 1*/f noise in continuous thin gold films*, Physica, **45,** 386–92, 1969.
2. J L Vossen, *Screening of metal film defects by current noise measurement*s, Appl. Phys. Lett, **23** 287–9, 1973.
3. G. Bertotti , M. Celasco, F. Fiorillo and P. Mazzetti, *Thermal equilibrium properties of vacancies in metal through current noise measurements*, J. Appl. Phys. **50,** 6948, 1979.

4. C Ciofi, B Neri, *Low-frequency noise measurements as a characterization tool for degradation phenomena in solid-state devices*, Journal of Physics D **33**, R199-R216, 2000
5. T Boutchacha, G Ghibaudo, G. Guégan and T. Skotnicki, *Low frequency noise characterization of 0.18μm Si CMOS transistors*, Microelectronics and Reliability, **37**, 1599-1602, 1997.
6. R. Landauer, *The noise is the signal*, Nature **392**, 658-659, 1998
7. G Iannaccone, G Lombardi, M Macucci, B Pellegrini, *Enhanced shot noise in resonant tunnelling*, Phys. Rev. Lett. **80,** 1054–1057, 1998
8. B Neri, C Ciofi, V Dattilo, *Noise and Fluctuations in Submicrometric Al-Si Interconnect Lines*, IEEE Trans. Electr. Dev. **44**, 1454-1459, 1997.
9. F Crupi, G Iannaccone, B Neri, C Ciofi, S Lombardo, *Shot noise partial suppression in the SILC regime*, Microelectron. Reliab. **40**, 1605-1608, 2000.
10. F Crupi, G Iannaccone, C Ciofi, B Neri, S Lombardo, C Pace, *Low frequency noise in unstressed/stressed thin oxide metal-oxide-semiconductor capacitors*, Solid State Electronics, **46**, 1807-1813 2002.
11. A Diligenti, B Neri, P E Bagnoli, A Barsanti, M Rizzo, Electromigration detection by means of low-frequency noise measurements in thin film interconnections, IEEE Trans. El.Dev.Lett., **6**, 606-608, 1985.
12. T M Chen, T P Djeu, R D Moore, *Electromigration and 1/f noise of aluminum thin films*, Proc. 1985 IEEE Rel.Phy. Symp., 87-92, 1985.
13. A Diligenti et al., *A study of electromigration in aluminum and aluminum-silicon thin film resistors using noise technique*, Solid State El., **32**, 11-16, 1989.
14. J G Cottle, N S Klonaris, M Bordelon, *$1/f^{\alpha}$ noise and fabrication variation of TiW/Al VLSI interconnections*, IEEE Electron Device Lett.,**11**, 523-526, 1990.
15. Z N Celik-Butler, Min Ye, *Prediction of Electromigration failure in W/Al-Cu multilayered metallization by 1/f noise measurements*, Solid State Electronics, **35**, 1209-1212, 1992.
16. C Ciofi, M De Marinis, B Neri, *Ultralow-Noise PC-Based Measurement System for the Characterization of the Metallizations of Integrated Circuits*, IEEE Trans. Instr. Meas., **46**, 798-793, 1997.
17. C Ciofi, I Ciofi, S Di Pascoli, B Neri, *Temperature controlled oven for low noise measurement systems*, IEEE Trans. Instr. Meas. **49**, 546-549, 1999.
18. P Olivo, T N Nguyen, B Ricco, *High-field-induced degradation in ultra-thin SiO2 films*, IEEE Trans. Electr. Dev., **35**, 2259-2267, 1988.
19. S Takagi, N Yasuda, A Toriumi, *A new I-V model for stress-induced leakage current including inelastic tunneling*, IEEE Trans. Electron. Dev., **46**, 348-354, 1998.
20. K Okada, K Taniguchi, *Electrical stress-induced variable range hopping conduction in ultrathin silicon dioxides*, Appl. Phys. Lett., **70**, 351-353, 1997.
21. M Depas, T Nigam, M. Heyns, *Soft breakdown of ultra-thin gate oxide layers*, IEEE Trans. Electron. Dev., **43**, 1499-1504, 1996.
22. F Crupi, R Degraeve, G Groeseneken, T Nigam, H E Maes: *Characteristics and correlated fluctuations of the gate and substrate current after oxide soft-breakdown*, Ext. Abst of the 1998 SSDM.
23. T Tomita, H Utsunomiya, T Sakura, Y Kamakura, K Taniguhci, *A new soft breakdown model for thin thermal SiO2 films under constant current stress*, IEEE Trans. Electron. Dev., **46**, 159-164, 1999.
24. B E Weir, P J Silverman, D Monroe, K S Krisch, M A Alam, G B Alers, T W Sorsch, G L Timp, F Baumann, C T Liu, T Ma, D Hwang, *Ultra-thin gate dielectrics: they break down, but do they fail?*, IEDM Tech. Dig., 73-76, 1997.
25. R Degraeve, G Groeseneken, R Bellens, M Depas, H E Maes, *A consistent model for the thickness dependence of intrinsic breakdown in ultra-thin oxides*, IEDM Tech. Dig., 863, 1995.
26. G Ghibaudo; O Roux-dit-Buisson, *Low frequency fluctuations in scaled-down silicon CMOS devices: status and trends*, Proc.ESSDERC 94, 693-700, 1994.
27. E.Miranda, J.Sune, et al. *Soft breakdown fluctuation events in ultrathin SiO2 layers*, Applied-Physics-Letters. **73**, 490-2,1998.
28. O Roux et al. *Investigation of drain current RTS noise in small area silicon MOS transistors*, Microelectronic-Engineering, **15**, 547-50, 1991.
29. R Rofan, C Hu, *Stress-Induced Oxide Leakage*, IEEE Electron Dev. Let., **12**, 632-634, 1991.
30. F Crupi, B Neri, S Lombardo, *Pre-breakdown in thin oxide films*, El.Dev. Letters., **21**, 319-321, 2000.
31. F Crupi. C Ciofi, C Pace, G Iannaccone, B Neri, *Noise as a probe of the charge transport mechanisms through thin oxides in MOS structures*, Fluctuation and Noise Letters, **1**, L61-L64, 2001.

32. C Ciofi, F Crupi, C Pace, G Scandurra, M Patanè, *A new circuit topology for the realization of very low noise, wide bandwidth transimpedance amplifier,* submitted to IEEE Trans. Instr. Meas.
33. C Ciofi, R Giannetti, V Dattilo, B Neri**,** *Ultra Low-Noise Current Sources,* IEEE Trans. Instr. Meas**. 47**, 78-81, 1998.
34. C Ciofi, M De Marinis, B Neri, *Wafer Level Measurement System for SARF Characterization of Metal Lines,* Microelectron. Reliab. **36**, 1851-1855, 1996.
35. L Baracchino, G Basso, C Ciofi, B Neri, *Ultralow-Noise, Programmable, Voltage Source*, IEEE Trans. Instr. Meas. **46**, 1256-1261, 1997.
36. C Ciofi, *High Precision, Integrable, Static Memory for Analog Signals, Alta Frequenza* **8**, 63-66, 1996.
37. G Scandurra C Ciofi, *R/βR Ladder Networks for the Design of High Accuracy Static Analog Memory*, to appare on IEEE Trans. Circ. Syst. I
38. C Pace, C Ciofi, F Crupi *Very low noise, high accuracy, programmable voltage reference*, to appare in *IEEE Trans. Instr. Meas*
39. V Dattilo, B Neri, C Ciofi, *Low frequency noise evolution during lifetime tests of lines and vias subjected to electromigration*, Microelectron. Reliab. **40**, 1323-1327, 2000
40. M Macucci, B Pellegrini *Very sensitive measurement method of electron device current noise*, IEEE Trans. Instrum. Meas., **40**, 7-12, 1991
41. M Sampietro, L Fasoli, and G Ferrari *Spectrum analyzer with noise reduction by cross correlation technique on two channels*, Rev. Sci. Instrum., **70** , 2520-2525, 1999
42. E Rubiola, V Giordano *A correlation-based noise measrurement scheme showing sensitivity below the thermal floor*, Proceedings of International Conference on Noise in Physical Systems and 1/f Fluctuations. Hong Kong, 483-486, 1999
43. C Ciofi, F Crupi, C Pace, *A new method for high sensitivity noise measurements,* IEEE Trans. Instr. Meas., **51**, 656-659, 2002